Electric-field enhancement of dielectronic recombination from a continuum of finite bandwidth

J. G. Story,* B. J. Lyons, and T. F. Gallagher
Department of Physics, University of Virginia, Charlottesville, Virginia 22901
(Received 3 October 1994)

A small electric field is shown to increase the dielectronic recombination, via autoionizing Rydberg states, of an electron from a continuum of finite bandwidth. The continuum of finite bandwidth is a broad autoionizing state which is part of a series converging to a higher limit, and the field enhancement of the rate occurs because the field converts the nl Rydberg states to nk Stark states, increasing the number of contributing recombination paths. The experimental results are in excellent agreement with the predictions of an isolated resonance approximation treatment and show clearly both the positive effect of Stark mixing and the negative effect of field ionization on dielectronic recombination.

PACS number(s): 34.80.Kw, 32.60.+i

I. INTRODUCTION

Dielectronic recombination (DR), the recombination of an ion and an electron via autoionizing states, proceeds largely through autoionizing Rydberg states [1]. For example, in zero-field the DR of Mg^+ ground-state ions and 4.5-eV electrons proceeds via the process

$$Mg^+3s+e^-\rightarrow Mg\ 3pnl\rightarrow Mg\ 3snl+h\nu\ . \quad (1)$$

Since the Rydberg states play such a crucial role in DR and they are affected by small electric fields, the DR rate can be substantially altered by small fields, as first pointed out by Jacobs, Davis, and Kepple [2,3]. There are two effects of a field. First, the field converts the zero-field nl Rydberg states to nk Stark states and redistributes the large autoionization rates of the low-l states over the Stark states, raising the number of participating states and the DR rate. Second, the field ionizes the high-n Rydberg states, reducing the DR rate. The net effect of a field on the DR rate can be either positive or negative depending on the field.

The first mentioned effect of a field was largely ignored until Belic *et al.* [4] measured DR in Mg, the process of Eq. (1), using crossed Mg^+ and e^- beams. They observed a DR signal five times larger than expected from prior calculations [5]. In their experiment the recombination took place in a magnetic field which produced a motional electric field of 24 V/cm and the product neutral Mg atoms were separated from the primary Mg^+ beam by a 36-V/cm separating field downstream from the collision region. While the negative effect of the separating field, to remove high-lying Rydberg states from the Dr product channel, had been taken into account, the positive effect due to the motional field's altering the autoionization rates had not been considered. When it was properly taken into account the measured and observed DR signals were in reasonably good agreement [6].

In later experiments three values of the motional field in the collision region were used: 3.6, 7.2, and 23.5 V/cm, while keeping the separating field at 40 V/cm to allow a more systematic check of the effect of the field in the collision region on DR [7–9]. These experiments showed that the DR signal increased as the field in the collision region was increased. Since the negative effect of a 40-V/cm field was always present, as long as the field in the collision region was less than 40 V/cm, increasing it should increase the DR signal. Both the magnitude of the observed signals and the final product Mg state distributions of these systematic experiments agreed reasonably well with calculations of several groups, suggesting that the understanding of DR in fields was on firm ground [10–12].

An interesting question which the experiments and most of the calculations have not addressed is, at what field is the DR rate maximized, irrespective of how the DR is observed? Calculations for DR of Mg^+ and Ca^+ have addressed this issue, and they show maxima in the DR rates at fields of 1–2 V/cm, fields an order of magnitude lower than used in the Mg experiments [12,13]. At 1–2 V/cm the calculated DR rates are three times larger than the zero-field rates, and at fields of a few hundred V/cm the rates have decreased to the zero-field rates.

To show explicitly the effects of small fields on DR we have examined the effects of small electric fields on DR from a continuum of finite bandwidth [14]. All the experimental parameters, such as the energy of the incident electron and the electric field, can be carefully controlled. The field produces an increase in the recombination rate which we show to be in good quantitative agreement with the calculated rates. In the following sections of this paper we first review the essential notions of DR and show the similarity between true DR and DR from a continuum of finite bandwidth. We then describe our experimental method, present the results, and compare our results to theoretical predictions and the results obtained in the Mg DR calculations.

*Present address: University of Missouri, Rolla, MO 65401.

II. DIELECTRONIC RECOMBINATION FROM A CONTINUUM OF FINITE BANDWIDTH IN AN ELECTRIC FIELD

Although DR can be treated more elegantly by quantum-defect theory [15,16], the isolated resonance approach provides a more intuitive picture, and we use it here. As shown by Eq. (1), DR of a singly charged ion and an electron can be envisioned as a two step process. First an electron excites an ion and is captured by it, forming an autoionizing state of the neutral atom. Then the autoionizing state radiatively decays to a bound state, completing the process. For the Ba atom, which we have studied, dielectronic recombination of a ground-state Ba^+ ion and an electron can occur via the autoionizing $6pnd$ Rydberg states by a process analogous to that of Eq. (1). Explicitly,

$$Ba^+ 6s + e^- \rightarrow Ba\ 6pnd \rightarrow Ba\ 6snd + h\nu \ . \tag{2}$$

The contribution of a particular nl autoionizing state to the DR rate is its rate of capture of free electrons from the Ba^+ $6s$ continuum multiplied by the branching ratio for fluorescence. Here n and l are the principal and orbital angular momentum quantum numbers of the Rydberg electron. Since the capture rate is proportional to the autoionization rate to the $6s$ continuum, the contribution to the total DR rate of the nl state is given by

$$S(nl)=\frac{\beta\Gamma_s(nl)A(nl)}{\Gamma_s(nl)+\Gamma_d(nl)+A(nl)} \ , \tag{3}$$

where β is a constant and $\Gamma_s(nl)$ and $\Gamma_d(nl)$ are the autoionization rates of the $6pnl$ state to the Ba^+ $6s$ and $5d$ continua. $A(nl)$ is the $6pnd \rightarrow 6snd$ fluorescent decay rate. Since it is the Ba^+ $6p \rightarrow 6s$ decay rate with a spectator electron it is a constant: $A(nl)=A$ and $A=3.88\times10^{-9}$ a.u. [17]. The total DR rate is obtained by multiplying $S(nl)$ by the degeneracy factor $(2l+1)$ and summing over n and l.

To understand how a field enhances DR we need only know the scalings of the rates of Eq. (3). To an excellent approximation, $\Gamma_s(nl)=\gamma_s(l)n^{-3}$ and $\Gamma_d(nl)=\gamma_d(l)n^{-3}$, where $\gamma_s(l)$ and $\gamma_d(l)$ both decrease rapidly with l. Making these substitutions in Eq. (3) yields

$$S(nl)=\beta\frac{\gamma_s(l)n^{-3}A}{\gamma_s(l)n^{-3}+\gamma_d(l)n^{-3}+A} \ . \tag{4}$$

For a given value of l there is typically a value of n, n_l, for which the autoionization and radiative decay rates are equal, i.e., $\Gamma_s(nl)+\Gamma_d(nl)=A$. For n less than n_l, $S(nl)\approx\beta\gamma_s(l)A/[\gamma_s(l)+\gamma_d(l)]$, a constant. For n greater than n_l the DR rate is given by $S(nl)\approx\beta\gamma_s(l)n^{-3}$. While individual states of $n>n_l$ contribute relatively little to DR, in the limit of large n_l, it is easy to show that, together, states of $n>n_l$ contribute half as much to the DR rate as the states of $n<n_l$. Consequently, a reasonable estimate of the total DR rate of all n states of this l is obtained by counting the states for which $\Gamma_s(nl)+\Gamma_d(nl)>A$ and multiplying by $\frac{3}{2}$. If we sum over all values of l we obtain the total DR rate, given by

$$S\approx\frac{3\beta NA}{2} \ , \tag{5}$$

where N is the number of states for which $\Gamma_s(nl)+\Gamma_d(nl)>A$. Since autoionization rates decrease with l, as l is increased n_l decreases, and for some l the autoionization rates are always smaller than the radiative decay rate. For this and all higher values of l the contribution to the total DR rate is negligibly small.

An electric field increases the DR rate in the following way. For many n states it is the case that low-l states have autoionization rates far in excess of the fluorescence rate while for high-l states the situation is reversed. In this case the high-l states contribute little to DR. In the presence of an electric field l is no longer a good quantum number, although m is. The nl states of a given m are converted to nk Stark states of the same m and the rapid autoionization rates of the low-l states are spread more or less evenly over all the Stark states, producing autoionization rates in excess of the fluorescent decay rates in all the Stark states. The increased number of states with autoionization rates exceeding the radiative rate leads to an increased DR rate. No states with high m have low l and they do not contribute significantly to DR with or without a field. In zero-field states of high l but low m do not contribute to DR, but in a field they are converted to Stark states and contribute to DR. The contribution of a field to the DR rate is not entirely positive. Field ionization cuts off the contribution of high-lying Rydberg states. For low values of m, the quantum number cutoff occurs at the classical ionization limit, at principal quantum number $n_c=1/(2E^{1/4})$.

We have investigated the electric-field enhancement of dielectronic recombination from a continuum of finite bandwidth, which is a broad autoionizing state degenerate with a Rydberg series of autoionizing states converging to a lower excited state of the ion [4]. Before considering electric-field effects we wish to show the similarity of DR from a continuum of finite bandwidth to true DR. The system we have chosen to study is shown in Fig. 1. The broad Ba $6p_{3/2}11d$ state is degenerate with the high-lying Ba $6p_{1/2}nd$ states and the Ba $6p_{1/2}\epsilon d$ continua just above the Ba^+ $6p_{1/2}$ limit. The broad $6p_{3/2}11d$ state plays the role of a continuum of finite bandwidth. Ba atoms are excited to the $6p_{3/2}11d$ state and electrons from this continuum of finite bandwidth induce the Ba^+ $6p_{3/2}\rightarrow6p_{1/2}$ transition and are captured into the $6p_{1/2}nd$ states. They can then decay radiatively to the $6s_{1/2}nd$ states or decay back to the $6p_{3/2}11d$ state or the real $6s\epsilon l$ or $5d\epsilon l'$ continua. The rate of radiative decay via a $6p_{1/2}nd$ state, the recombination rate, is given by

$$S(nd)=\beta\frac{R(nd)A(nd)}{R(nd)+\Gamma(nd)+A(nd)} \ , \tag{6}$$

where $R(nd)$ is the rate of transitions from the $6p_{1/2}nd$ state to the $6p_{3/2}11d$ state, $\Gamma(nd)$ is the autoionization rate of the $6p_{1/2}nd$ state to the real continua, and $A(nd)$ is the fluorescent decay rate of the $6p_{1/2}nd$ state to the $6s_{1/2}nd$ state. As before $A(nd)=A$. $R(nd)$ and $\Gamma(nd)$ are given by $R(nd)=rn^{-3}$ and $\Gamma(nd)=\gamma n^{-3}$ [18,19].

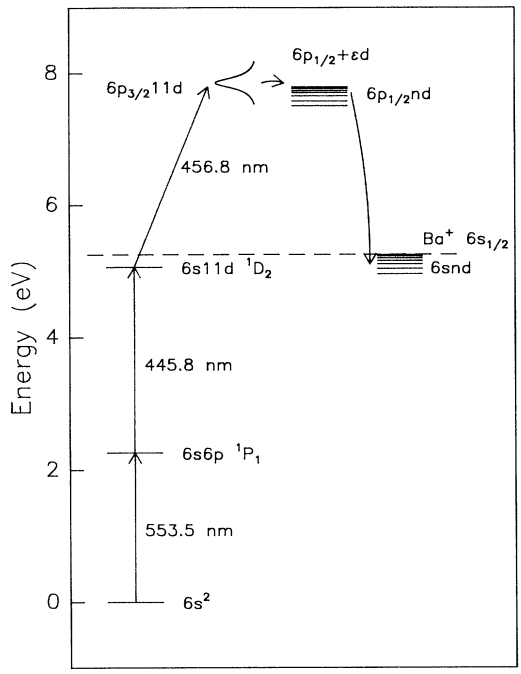

FIG. 1. Three lasers are used to excite the $6p_{3/2}11d$ state. The first two lasers excite the $6s11d\ ^1D_2$ Rydberg state. The third laser is tuned near the Ba^+ $6s_{1/2}$ to $6p_{3/2}$ transition to excite the core electron to produce $6p_{3/2}11d$ states. The broad $6p_{3/2}11d$ state is degenerate with the $6p_{1/2}nd$ Rydberg series and acts as a degenerate continuum of finite bandwidth. Dielectronic recombination from this continuum of finite bandwidth occurs when an atom makes a transition from the $6p_{3/2}11d$ state to the $6p_{1/2}nd$ state followed by fluorescent decay of the $6p_{1/2}$ ion which leaves the atom in a high-lying bound Rydberg state.

Using these scalings we can recast Eq. (6) into a form identical to Eq. (4). Explicitly,

$$S(nd)=\frac{\beta r n^{-3} A}{r n^{-3}+\gamma n^{-3}+A} . \tag{7}$$

It is apparent that Eq. (7) has the same form as Eq. (4). Consequently the process described by Eqs. (6) and (7) is dielectronic recombination from a continuum of finite bandwidth. This process has been examined in zero field by Story, Van Woerkom, and Cooke and shown to have small but finite rates [20]. There is a difference between our experiment and true DR. In our experiment the incoming electron is a d wave of known m, while in true DR all partial waves are present. Since low-m states are expected to contribute much of the true DR rate, we do not expect this difference to be particularly significant.

Applying a small electric field converts the $6p_{1/2}nl$ states to the the $6p_{1/2}nk$ Stark states, but does not affect the $6p_{3/2}nd$ state, and the recombination rate via a $6p_{1/2}nk$ Stark state is given by an expression identical to Eq. (6). Explicitly,

$$S_E(nk)=\frac{\beta R(nk) A(nk)}{R(nk)+\Gamma(nk)+A(nk)} , \tag{8}$$

where β is the same constant as in Eq. (6), $R(nk)$ is the transition rate from the $6p_{1/2}nk$ state to the $6p_{3/2}11d$ state, $\Gamma(nk)$ is the autoionization rate to the continua, and $A(nk)=A$ as before.

We can write Eq. (8) in a form analogous to that of Eq. (7) by using the n scalings of $R(nk)$ and $\Gamma(nk)$. Since the $6p_{3/2}11d$ state is unaffected by the electric fields we apply, it is only coupled to the nd components of the $6p_{1/2}nk$ Stark states, and $R(nk)=rn^{-4}$. $R(nk)$ is the $6p_{1/2}nd$-$6p_{3/2}11d$ transition rate spread over all the $6p_{1/2}nk$ Stark states. For similar reasons $\Gamma(nk)=\gamma_E n^{-4}$ [21], where the coefficient γ_E is related to $\gamma(l)$ by [19,20]

$$\gamma_E=\sum_{l=0}^{n-1}\gamma(l) . \tag{9}$$

In this discussion we have implicitly assumed that $m=0$. It is worth noting that the results of the analysis would not be noticeably different for $m\leq 3$ since the Stark state autoionization rate is derived in large part from the $6p_{1/2}nf$ states [21]. With the n scalings Eq. (8) becomes

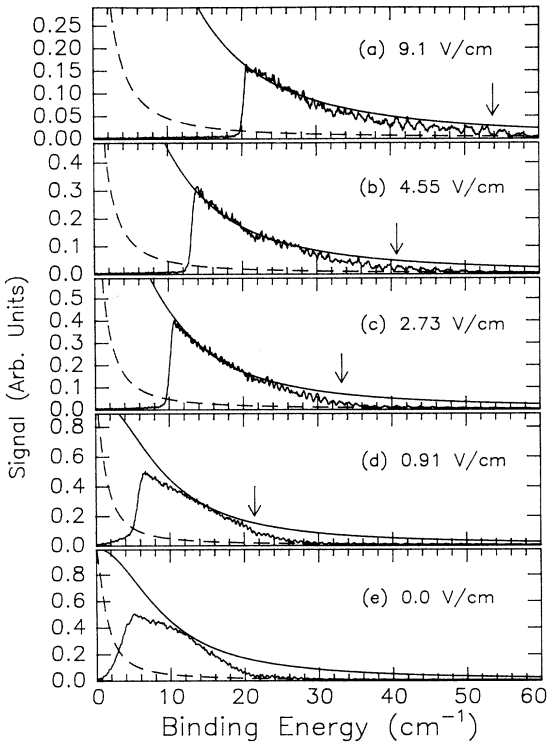

FIG. 2. The field ionization signal versus tuning of the third laser relative to the $6p_{1/2}$ ionization limit is shown for applied static fields of (a) 9.1, (b) 4.55, (c) 2.73, (d) 0.91, and (e) 0.0 V/cm. The field ionization signal represents atoms which have undergone recombination via $6p_{1/2}nd$ or $6p_{1/2}nk$ states. The lower curve (— — —) is the calculated zero-field recombination signal. The upper smooth curve (——) is the calculated Stark mixed recombination signal. The arrows represent the calculated Inglis-Teller limits given by $W_I=(3E)^{5/2}/2$. The data are normalized to the calculated curves in (b) between 15 and 25 cm^{-1}.

$$S_E(nk)=\frac{\beta r n^{-4} A}{r n^{-4}+\gamma_E n^{-4}+A} . \quad (10)$$

To compare our experimental results to the DR rates per state of Eqs. (7) and (10) we first convert them to DR rates per unit energy. Explicitly, Eq. (7) becomes

$$\frac{dS}{dW}=S(nd)\frac{dn}{dW}=\frac{\beta r A}{r n^{-3}+\gamma n^{-3}+A} , \quad (11)$$

where we have used for the number of states per unit energy $dn/dW=n^3$. Using these scalings, as $n\to\infty$, $dS/dW\to\beta r$ and this sets the experimental scale. For small n, $dS/dW\simeq\beta r n^3/[r+\gamma(d)]=\beta r(2W)^{-3/2}$. To evaluate Eq. (11) we use the experimentally determined values $r=0.05$ and $\gamma=0.05$ [18,19,22] and in Fig. 2 we show plots of dS/dW as broken lines.

We need to develop the analog of Eq. (11) for the case in which there is a field present. We assume complete Stark mixing of all levels of a given m and ignore field ionization. With these approximations we can write the electric-field analog of Eq. (11) for $m=0$ as

$$\frac{dS_E}{dW}=S(nk)\frac{dn}{dW}=\frac{\beta r A}{r n^{-4}+\gamma_E n^{-4}+A}=\frac{\beta r A}{4rW^2+\delta W^2+A} . \quad (12)$$

Equation (12) is similar to Eq. (11), but there are several important differences. First, the number of $m=0$ Stark states per unit energy is n^4, not n^3. As $n\to\infty$, $dS_E/dW=\beta r$, the same value as in zero field. However, for lower n, where $R(nk)$ and $\Gamma(nk)$ exceed A, dS_E/dW in the field exceeds dS/dW in zero field, as shown by the smooth solid line of Fig. 2. To evaluate dS_E/dW we use the measured value of $\gamma_E=0.53$ [21].

III. EXPERIMENTAL APPROACH AND OBSERVATIONS

The experiment was done by exciting Ba atoms in a beam to the broad $6p_{3/2}11d$ state and measuring the number of atoms which underwent radiative stabilization and were left in bound $6snd$ Rydberg states. The number of stabilized atoms was measured as a function of both the precise excitation energy within the $6p_{3/2}11d$ state and the applied electric field.

Using the isolated core excitation approach shown in Fig. 1 we excited the Ba atoms using three 5-ns dye lasers which were pumped by the third harmonic of a 9-ns Q-switched Nd:YAG laser. The bandwidth of the third laser, which drove the Ba^+ $6s_{1/2}$ to $6p_{3/2}$ transition, was 0.38 cm^{-1}. The relative frequency of the third laser was measured using an étalon and the absolute frequency was measured by matching the low-n data, where the $6p_{1/2}nd$ Rdyberg states could be clearly resolved, to the known positions of the $6p_{1/2}nd$ states, which have a quantum defect of 2.75. The three lasers used in the excitation were overlapped and crossed an effusive beam of Ba atoms in the interaction region between two capacitor plates spaced by 1.1 cm. Typically the lasers were polarized parallel to the electric field, but we observed no effect upon rotating the polarizations, suggesting that for $m\leq 2$ the results are independent of m, as suggested in the preceding section. Approximately 100 ns after the laser pulses a 95-V pulse was applied to the capacitor plates to field ionize any high Rydberg states produced by the stabilization process. A screen mesh in the top plate allowed the passage of electrons which were then detected by a pair of microchannel plates. The data were taken by recording the field ionization signal as the wavelength of the third laser was swept with the static field held constant.

The data shown in Fig. 2 were obtained by scanning the third laser over that part of the $6p_{3/2}11d$ state which overlaps in energy the high-lying $6p_{1/2}nd$ states for nominal static fields of 0, 2.73, 4.55, and 9.1 V/cm. In the figure, the stabilization signals are plotted versus the binding energy of the $6p_{1/2}nd$ states. All of the experimental signals of Fig. 2 are normalized to the same scale, with the normalization point being the 4.55-V/cm trace between binding energies of 15 and 25 cm^{-1}. We use the convention that binding energies are positive. Note that the vertical scales are expanded for higher electric fields and that there is more stabilization signal at low fields than at high fields.

The broken line is the stabilization per unit energy in zero field calculated using Eq. (11). The smooth solid line is the stabilization per unit energy, assuming complete Stark mixing and ignoring field ionization, calculated from Eq. (12). The arrows are at the binding energy $W_I=(3E)^{5/2}/2$, the Inglis-Teller limit, where the $m=0$ Stark manifolds of adjacent n overlap and Stark mixing of low-l states with large quantum defects should be com-

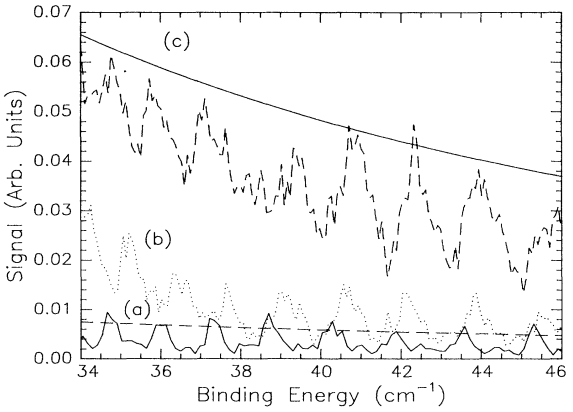

FIG. 3. The field ionization signal versus tuning of the third laser relative to the $6p_{1/2}$ ionization limit is shown for (a) 0, (b) 2.73, (c) 9.1 V/cm. In (a), the zero-field case, the positions of the nd states are evident. In (b), with 2.73 V/cm, the positions of the resonances are shifted, with the amount of shift dependent on n. In (c), with 9.1 V/cm, the broad structures are the Stark manifolds. The upper smooth curve (——) is the calculated Stark mixed recombination signal and the lower smooth curve (— — —) is the calculated zero-field recombination signal.

plete. For all nonzero applied fields and binding energies less than the classical field ionization limit $W_C = 2\sqrt{E}$, there are no stable Rydberg states due to field ionization and there is no stabilization signal. For binding energies greater than W_C but less than W_I, the stabilization signal falls on the calculated Stark mixed curve, and as the binding energy is further increased the signal drops to the calculated zero-field stabilization curve. The nominal zero-field signal does not fall on the calculated zero-field curve. Between the binding energies of 5 and 15 cm^{-1} it lies on the Stark mixed curve, due to stray fields. At smaller binding energies it is cut off, due to field ionization, and at a binding energy of 18 cm^{-1} it has fallen halfway to the zero-field curve. These energies are consistent with a stray field of 0.7 V/cm.

The data of Fig. 2 show clearly that, as predicted [2,12], even small fields significantly increase the DR rate. Recording the data with higher resolution shows that it is the conversion of the zero-field nl states to nk Stark states which is responsible for the increase. In Fig. 3 we show high-resolution scans of the third laser over the range of binding energy from 34 to 46 cm^{-1}, which corresponds to $n = 52$ to 60, for applied fields of 0.0, 2.73, and 9.1 V/cm. Over this range the zero-field data are virtually unaffected by stray electric fields. In Fig. 3(a) the zero-field $6p_{1/2}nd$ states are clearly visible and the data lie near the calculated zero-field curve. With a field of 2.73 V/cm at high binding energies the spectral features are still near the zero-field $6p_{1/2}nd$ features of Fig. 3(a), but at low binding energy the observed structure shows the evolution to Stark manifolds and the data lie significantly above the calculated zero-field curve. Finally, at 9.1 V/cm the spectrum has evolved into a Stark spectrum, in which only outlines of the entire manifolds can be discerned and the signal level approaches the calculated Stark mixed curve.

In Fig. 2 all the experimental traces but the zero-field one, which is affected by stray fields, are in excellent agreement with the calculated curves. By integrating the calculated curves we can determine the total DR rate vs field. We integrate Eq. (12) from the classical ionization limit W_C to the Inglis-Teller limit W_I where the experimental signals fall halfway between the Stark mixed and zero-field curves. For larger binding energies we integrate Eq. (11), the zero-field rate. Explicitly,

$$S_E = \int_{W_C}^{W_I} \frac{\beta r A dW}{r n^{-4} + \gamma_E n^{-4} + A} + \int_{W_I}^{\infty} \frac{\beta r A dW}{r n^{-3} + \gamma n^{-3} + A} . \tag{13}$$

For $E = 0$ only the second integral contributes. Figure 4 is a plot of S_E/S_0 which shows explicitly the enhancement of the total DR rate by the field. The maximum enhancement is a factor of 2.2 and occurs at 0.3 V/cm. The experimental values, obtained by integrating the signals, are also plotted. The normalization point is the 4.55-V/cm field data as in Fig. 2. The nominal zero-field point is plotted at 0.7 V/cm, the stray field inferred from Fig. 2. As shown, the data are in good agreement with the calculated values.

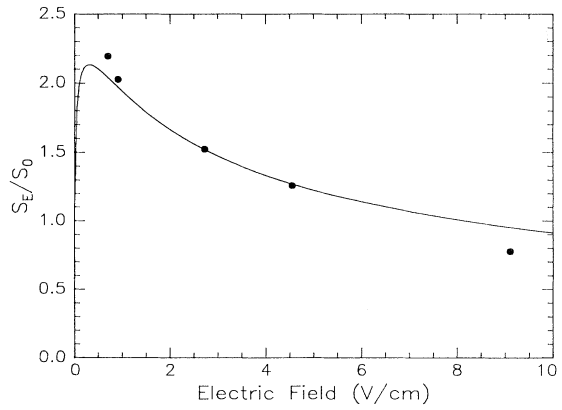

FIG. 4. Calculated and observed enhancement ratio S_E/S_0 vs applied field. The nominal zero-field point is plotted at 0.7 V/cm to account for the presence of stray fields.

IV. DISCUSSION AND CONCLUSION

It is useful to compare our results to those previously obtained for Mg, where theory and experiment are in reasonably good accord in their region of overlap. Unfortunately, we cannot compare our results directly to the experimental results because of the large separating field. We can, however, compare them to the Mg calculations. The enhancement factors calculated for Mg at 1, 5, 20, and 100 V/cm are 2.9, 2.4, 2.1, and 1.5 [12]. Although the field values are too far apart to locate accurately the maximum in the calculated enhancement factor, it is clear that the maximum value is approximately 3 and occurs at a field of approximately 1 V/cm. These results are quite close to ours, a maximum enhancement factor of 2.2 at 0.3 V/cm. Considering that the calculations are done for Mg, not Ba, and that in the Mg calculation the incoming electron is not constrained to be a d wave, we feel the argument is excellent. There is a significant difference though; the calculated Mg enhancement factor falls much more slowly with field than the values we have measured in Ba. Since lower-n states contribute more heavily at higher fields, we suspect that at least some of the discrepancy between our results and the Mg calculation is due to the finite bandwidth of our continuum, which excludes low-lying states.

The experimental results presented here show clearly both of the anticipated effects of electric fields on DR, the suppression of DR at high n by field ionization, and the enhancement of DR at low n due to stark mixing. Due to the competition between these two effects there exists a nonzero field at which there is a maximum DR rate. Further, the analysis of these experiments demonstrates that isolated resonance theories of DR in fields give quantitatively useful predictions.

ACKNOWLEDGMENTS

This work has been supported by the U.S. Department of Energy, Office of Basic Energy Sciences. It is a pleasure to acknowledge stimulating and helpful conversations with R. R. Jones and K. LaGattuta.

[1] A. Burgess, Astrophys. J. **139**, 776 (1964).
[2] V. L. Jacobs, J. Davis, and P. C. Kepple, Phys. Rev. Lett. **37**, 1390 (1976).
[3] V. L. Jacobs and J. Davis, Phys. Rev. A **19**, 776 (1979).
[4] D. S. Belić, G. H. Dunn, T. J. Morgan, D. W. Mueller, and C. Timmer, Phys. Rev. Lett. **50**, 339 (1983).
[5] K. LaGattuta and Y. Hahn, J. Phys. B **15**, 2101 (1982).
[6] K. LaGattuta and Y. Hahn, Phys. Rev. Lett. **51**, 558 (1983).
[7] G. H. Dunn, D. S. Belić, B. DePaola, N. Djurić, D. Mueller, A Müller, and C. Timmer, in *Atomic Excitation and Recombination in External Fields,* edited by M. H. Nayfeh and C. W. Clark (Gordon and Breach, New York, 1985).
[8] A. Müller, D. S. Belić, B. D. DePaola, N. Djurić, G. H. Dunn, D. W. Mueller, and C. Timmer, Phys. Rev. Lett. **56**, 127 (1986).
[9] A. Müller, D. S. Belić, B. D. DePaola, N. Djurić, G. H. Dunn, D. W. Mueller, and C. Timmer, Phys. Rev. Lett. A **36**, 599 (1987).
[10] C. Bottcher, D. C. Griffin, and M. S. Pindzola, Phys. Rev. A **34**, 860 (1986).
[11] K. LaGattuta, I. Nasser, and Y. Hahn, Phys. Rev. A **33**, 2782 (1986).
[12] K. LaGattuta, I. Nasser, and Y. Hahn, J. Phys. B **20**, 1565 (1987).
[13] K. LaGattuta, I. Nasser, and Y. Hahn, J. Phys. B **20**, 1577 (1987).
[14] J. P. Connerade, Proc. R. Soc. (London) **362**, 361 (1978).
[15] R. H. Bell and M. J. Seaton, J. Phys. B **18**, 1589 (1985).
[16] A. P. Hickman, J. Phys. B **17**, L101 (1984).
[17] A. Lindgard and S. E. Nielson, At. Data Nucl. Data Tables **19**, 543 (1977).
[18] F. Gounand, T. F Gallagher, W. Sandner, K. A. Safinya, and R. Kachru, Phys. Rev. A **27**, 1925 (1983).
[19] S. A. Bhatti, C. L. Cromer, and W. E. Cooke, Phys. Rev. A **24**, 161 (1981).
[20] J. G. Story, L. D. Van Woerkom, and W. E. Cooke, Phys. Rev. A **34**, 4508 (1986).
[21] R. R. Jones and T. F. Gallagher, Phys. Rev. A **39**, 4583 (1989).
[22] O. C. Mullins, Y. Zhu, E. Y. Xu, and T. F. Gallagher, Phys. Rev. A **32**, 2234 (1985).